

HUGHES RESEARCH LABORATORIES
Malibu, California

a division of hughes aircraft company

GPO PRICE \$ _____
CFSTI PRICE(S) \$ _____
Hard copy (HC) 3.00
Microfiche (MF) .65

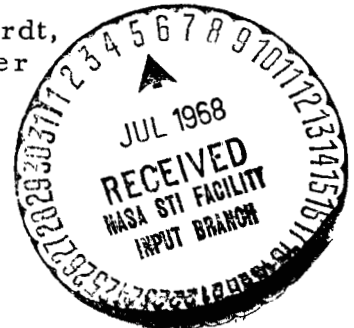
653 July 65

HIGH-TEMPERATURE LM CATHODE ION THRUSTERS

Quarterly Progress Report No. 1
5 February 1968 through 4 May 1968
Contract No. JPL 952131

J. Hyman, Jr., W. O. Eckhardt,
J. W. Pfeifer and J. A. Snyder
Plasma Physics Department

15 May 1968



"This work was performed for
the Jet Propulsion Laboratory,
California Institute of Technology,
as sponsored by
the National Aeronautics and Space Administration
under Contract NAS 7-100 (Task Order #RD-26)."

N 68-27741

FACILITY FORM 602

(ACCESSION NUMBER)

(PAGES)

(NASA CR OR TMX OR AD NUMBER)

(THRU)

(CODE)

(CATEGORY)

ABSTRACT

A 20-cm electron-bombardment thruster using an LM cathode was operated at a beam current $I_B = 550$ mA with a total source energy per ion $V_S = 250$ eV/ion at a mass utilization of 85% (V_S includes all power required to form the ions, since no vaporizer, cathode heater, or keeper power is required with the LM cathode). Measurements of Poiseuille flow of liquid mercury through a single-capillary stainless steel tube (0.0076 cm dia.) were linear and repeatable with pressure to within the experimental error of $\pm 5\%$ over the range 20-75 psia. A single-capillary flow impedance has been fabricated and is undergoing testing with a specially designed LM cathode. This combination may be capable of very high uniformity in the mercury flow rate. A new LM cathode has been fabricated which utilizes a linear-slit pool-keeping structure. LM cathode neutralizer development concentrated on establishing the limits of performance with copper as the permanently wettable metal (used to stabilize the position of the liquid surface) and comparing the performance of other materials. A thermally integrated 30-cm diameter permanent-magnet thruster has been designed which has a calculated weight of approximately 4.7 kg.

TABLE OF CONTENTS

I.	INTRODUCTION AND SUMMARY	1
II.	FLOW MEASUREMENT AND CONTROL	5
	A. Introduction	5
	B. Poiseuille Flow	7
	C. Single-Capillary Flow Measurements	10
	D. Single-Capillary Flow-Impedance Design	12
III.	LM CATHODE RESEARCH AND DEVELOPMENT	15
	A. Introduction	15
	B. Annular-Cathode Technology	17
	C. Linear-Slit Cathode	18
	D. Experimental Cathode with Single-Capillary Flow-Impedance	21
	E. LM Cathode Neutralizer	23
IV.	LM CATHODE THRUSTER OPTIMIZATION	27
	A. Introduction	27
	B. Modification of 20-cm PMT	28
	C. Design of 30-cm PMT	35
V.	CONCLUSIONS	39
VI.	RECOMMENDATIONS AND FUTURE PLANS	41
VII.	NEW TECHNOLOGY	43
VIII.	REFERENCES	45

LIST OF ILLUSTRATIONS

Fig. 1.	Schematic performance graph for an optimized thruster	6
Fig. 2.	Gas pressure mercury feed system	8
Fig. 3.	Circular and annular LM cathode geometries	9
Fig. 4.	Single-capillary flow impedance measurements	11
Fig. 5.	Experimental cathode with single-capillary flow impedance	15
Fig. 6.	Positions of mercury pool surface for an annular LM cathode	16
Fig. 7.	Annular LM cathode using a tantalum shim to establish the feed channel width	19
Fig. 8.	Linear-slit cathode	20
Fig. 9.	Flow fluctuations due to surface-tension forces	22
Fig. 10.	Schematic cross-section of LM cathode neutralizer	24
Fig. 11.	Present configuration of the modified 20-cm PMT	29
Fig. 12.	Experimental data for the modified 20-cm PMT with various baffle configurations	31
Fig. 13.	Experimental data for modified 20-cm PMT (present configuration)	34
Fig. 14.	Schematic drawing of the 30-cm PMT design	36

I. INTRODUCTION AND SUMMARY

Prior to the present effort, the technology of the LM cathode* and its operation had advanced to a stage where it could be used advantageously as the discharge cathode of a mercury electron-bombardment Kaufman³ thruster, and where it offered considerable promise for use as the neutralizer cathode of such thrusters. The feasibility of thruster life in excess of 10^4 hours had been demonstrated at Hughes Research Laboratories (HRL) when a 20-cm thruster equipped with an LM cathode was successfully tested for an accumulated 4000 hours.⁴ Following this test no erosion of the molybdenum cathode structure was evident, and no degradation of the cathode performance occurred. Furthermore, within the limits of experimental accuracy ($\pm 1\%$) time invariance of cathode and thruster characteristics had been demonstrated, as well as insensitivity to vacuum chamber environmental conditions. Annular LM cathodes had been operated at temperatures as high as 300°C in a satisfactory manner.⁵ This temperature is high enough to allow independence of the cathode from the thermal constraints of the thruster in space.^{5,6} Source energies per ion as low as $V_S = 400$ eV/ion (this is the total energy required to form an ion since no heater, vaporizer, or keeper power is required) had been demonstrated at a mass utilization of $\eta_m = 87\%$ in a 20-cm diameter thruster with a cathode temperature of 250°C , while the corresponding numbers for 300°C were $V_S = 443$ eV/ion at $\eta_m = 84\%$. Further, stable LM cathode operation in the neutralizer current range had been demonstrated,⁵ with attractive electron-to-atom emission ratios and power expenditures, at temperatures close to the equilibrium temperature of a neutralizer which is cooled only by radiation from its face.

When the thruster performance stated above was first reported by HRL⁴, it represented the best performance reported for any mercury electron-bombardment thruster. Since that time a class of highly optimized thrusters has been developed principally through the efforts at NASA Lewis Research Center (LeRC) on the 15-cm SERT II thruster system.^{7,8,9} In Reference 8, a discharge energy per ion of about 200 eV/ion is reported at a mass utilization of $\eta_m = 85\%$. The power required to heat the hollow cathode and the vaporizer were reported to result in an additional expenditure of 120 eV/ion,⁹ leading to a total source energy per ion $V_S = 320$ eV/ion at a mass utilization $\eta_m = 85\%$.

* For brevity, the gravity-independent, force-fed liquid metal cathode invented¹ and developed² at HRL will be referred to as the Liquid-Metal, or LM cathode. In this report the specific liquid metal is mercury.

The results obtained in the SERT II program at LeRC, and similar results obtained at HRL^{10, 11} and at JPL,¹² all supported the contention that an effort directed at discharge chamber optimization with respect to operation with an LM cathode would result in a significant increase in discharge chamber performance. Such improvements in discharge chamber efficiency, beside being a most worthwhile end in themselves, also result in reduced requirements on cathode performance. As the source energy per ion is reduced, the discharge current and consequently the cathode heat load $P_{K,th}$ decreases, as does the ratio of electron to atomic flux demanded from the cathode. Both of these reductions serve to relax the thermal constraints imposed on the cathode.

During the initial quarter of the present effort, an existing 20-cm diameter LM cathode thruster was modified to conform in magnetic field geometry (in first approximation) to the LeRC 15-cm SERT II thruster. Following a brief period of testing and modification the discharge chamber performance was improved to a level where it now matches or exceeds the performance reported for other optimized electron-bombardment thrusters. In thruster operation achieved during the last month, at a beam current $I_B = 550$ mA the total source energy per ion was $V_S = 250$ eV/ion at a mass utilization of $\eta_m = 85\%$.

To consolidate the benefits derived from these recent experimental advances and to reap the benefits indicated by past analytical studies⁵ the design and construction of a 30-cm diameter electron-bombardment mercury ion thruster has been undertaken which will be optimized for operation with an LM cathode. The thruster design, which is now complete, attempts to exploit the experience gained through recent development of thrusters at HRL, JPL, and LeRC. In addition to the optimization of discharge chamber performance, this thruster incorporates features necessary for thermal integration of the cathode with the overall thruster system while maintaining a light weight design. The weight of the overall thruster is calculated to be approximately 4.7 kg.

In parallel with the development of an electron-bombardment thruster which is optimized for use with the LM cathode, research and development continues on the cathode itself, as well as on many of the auxiliary components which are necessary to produce a workable thruster system. These areas of study include the neutralizer cathode, neutral mercury flow measurement and control, and techniques for electrical isolation between the thruster and the propellant storage tanks (the last area being the result of a recent related effort¹³).

Major improvements on the thruster cathode are being sought in regard to its specific thermal loading $V_{K,th}$ (the ratio of thermal cathode load to discharge current.) While LM cathodes have been

operated up to and above the required currents and electron-to-atom ratios⁵ at temperatures as high as 375°C, it is noted that this has been accompanied by a significant increase in specific thermal loading over the value $V_{K,th} \approx 2.5$ W/A observed in low-temperature operation. New techniques for the fabrication of high-temperature LM cathodes are described which are expected to permit operation at a specific thermal loading close to its low-temperature level. Such a reduction of $V_{K,th}$ will translate directly into higher thruster efficiency and lower thruster weight.

Current experiments involving Poiseuille flow in single capillary tubes indicate that it may be possible to exploit capillaries of small diameter (≈ 0.01 cm) for use as a flow impedance both to establish and to measure the very small mercury flow rates used with electron-bombardment thrusters.

II. FLOW MEASUREMENT AND CONTROL

A. Introduction

Under a previous contract⁴ we have demonstrated that it is possible to rely on measurements of beam current I_B as an accurate indication of neutral mercury flow rate I_a for automatically-controlled LM thruster operation. Operating data from highly optimized electron-bombardment thrusters indicate that some loss in thruster performance may result from reliance on indirect measurements of neutral flow rate.¹⁴ The reason for this can be understood by inspection of a graph of typical discharge chamber performance for a highly optimized thruster. Figure 1 is a schematic version of such a graph, showing source energy per ion (V_S) as a function of mass utilization (η_m) for a highly optimized thruster. It has the characteristic of possessing two saturation regions: one of almost constant V_S as a function of η_m , and one of almost constant η_m as a function of V_S .

It is reasonable to anticipate that missions will be planned in which the thrusters are normally required to operate in the transition between the two saturation regions. Thruster operation can be maintained automatically in this desired region only by knowledge of both η_m and V_S , because a deviation from this region along either one of the saturation lines does not result in a sufficient variation of the other parameter.

To determine η_m it is necessary to measure both the beam current I_B and the neutral mercury flow rate I_a since $\eta_m = I_B/I_a$. At present no technique exists which produces a direct instantaneous read-out of I_a . To measure the very low mercury flow rates which are required,^a only two techniques appear to offer promise at this time: the measurement of the rate of linear displacement of a mercury column, or the use of a calibrated mercury flow impedance which then reduces the problem to one of a pressure measurement (for which many techniques of direct, instantaneous read-out are available).

Positive displacement measurements have served for many years at HRL to produce mercury flow information with high accuracy. However, as presently embodied the technique requires several minutes for such accurate flow determinations. To obtain more rapid flow determinations from a positive displacement technique it is necessary to increase the rate of linear displacement for a given flow rate; in other words the mercury must move through a narrow channel. Recently, a liquid-mercury bubble isolator has been developed under another contract.¹³ In this device a hydrogen gas bubble is injected into an electrically insulating capillary tube through which mercury is flowing. After the bubble has travelled a prescribed distance, an electrical signal is generated and a new bubble is injected. This device is not only useful in providing electrical isolation between the two ends of the capillary tube (the hydrogen bubble interrupts the electrical continuity through the mercury column) but may also be used to provide a rapid readout of I_a since the velocity of the bubbles is directly proportional to flow rate.

E965-II

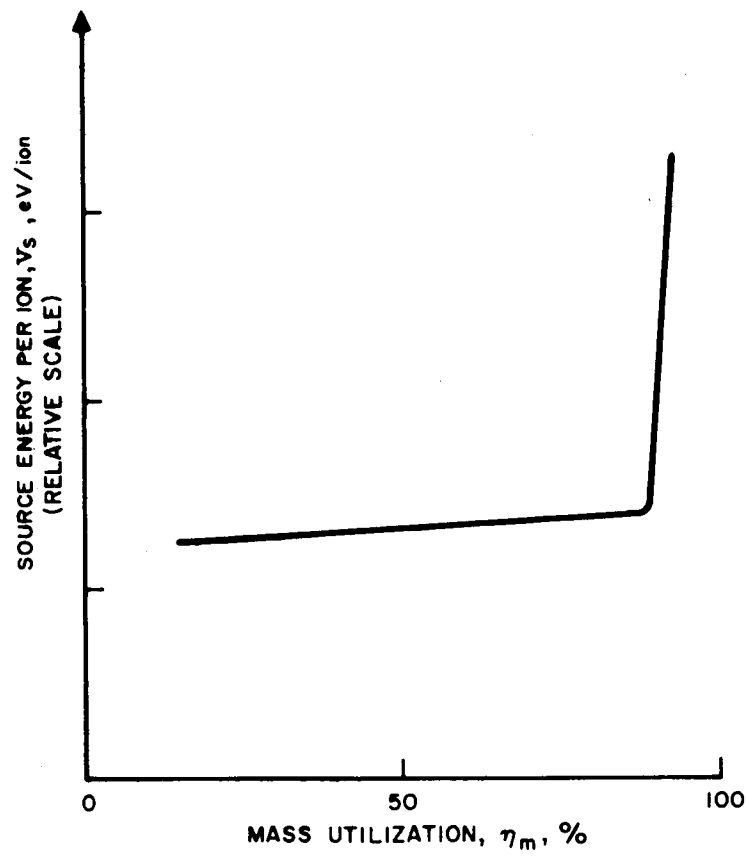


Fig. 1. Schematic performance graph for an optimized thruster.

Experiments conducted under the present contract indicate that it may be possible to construct a calibrated mercury flow impedance which is based on the principle of Poiseuille flow through a single capillary tube. The results of these experiments are reported below.

B. Poiseuille Flow

To replenish mercury liquid to the active cathode surface from a reservoir, a pneumatic system (shown schematically in Fig. 2) has been used, in which pressurized nitrogen is applied above a piston pressing on the mercury surface to serve as the driving force. The piston position is indicated with a dial indicator (calibrated to 0.001 in. or 0.0001 in.) contacting the top of the piston shaft. This serves as an indication of mercury consumption and yields an accurate measure of the flow rate. The mercury flow is regulated by passing mercury at the required pressure through a porous tungsten plug used as a flow impedance. This impedance is placed immediately upstream of a small plenum leading to the feed channel of the LM cathode pool-keeping structure as shown in Fig. 3.

Though the porous tungsten flow impedance has served with good results for many years, we have attempted in this quarter to establish a new technique for flow measurement and control which may offer several advantages for thruster operation. This method utilizes a single capillary tube to serve as the flow impedance. The flow rate through such a capillary is limited by viscous forces to a value given by Poiseuille's law.

$$\dot{V} = \frac{\pi D^4}{128 \eta L} (p_1 - p_2)$$

where \dot{V} is the volume flow rate, D is the diameter of a circular capillary tube, L is its length, η is the coefficient of viscosity of the liquid ($\eta_{\text{Hg}} = 1.55 \times 10^{-2}$ Poise) and p_1 and p_2 are respectively the upstream and downstream mercury pressures at the ends of the capillary tube. In convenient units this formula can be re-expressed as

$$I_a = 7.1 \times 10^8 \text{ A} \cdot \frac{(D/\text{cm})^4}{L/\text{cm}} \cdot (p_1 - p_2)/\text{psia},$$

where I_a is the current-equivalent of the atomic flow rate.

A potential advantage of single-capillary flow regulation is that the rate of flow is a linear function of the applied pressure and one which can easily be calculated. This permits the exact design of specific flow impedances to match the requirements of a given application. Past ex-

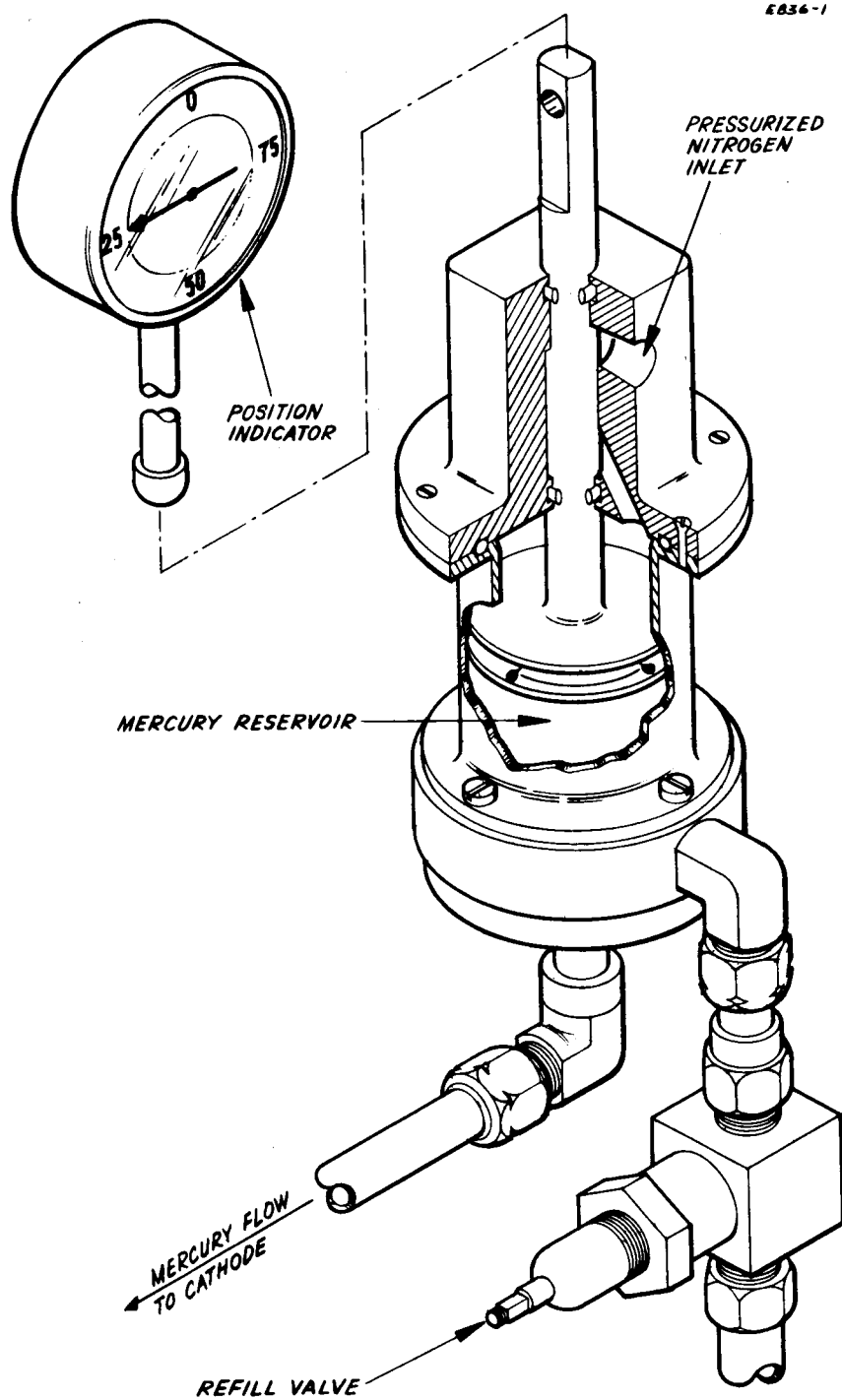
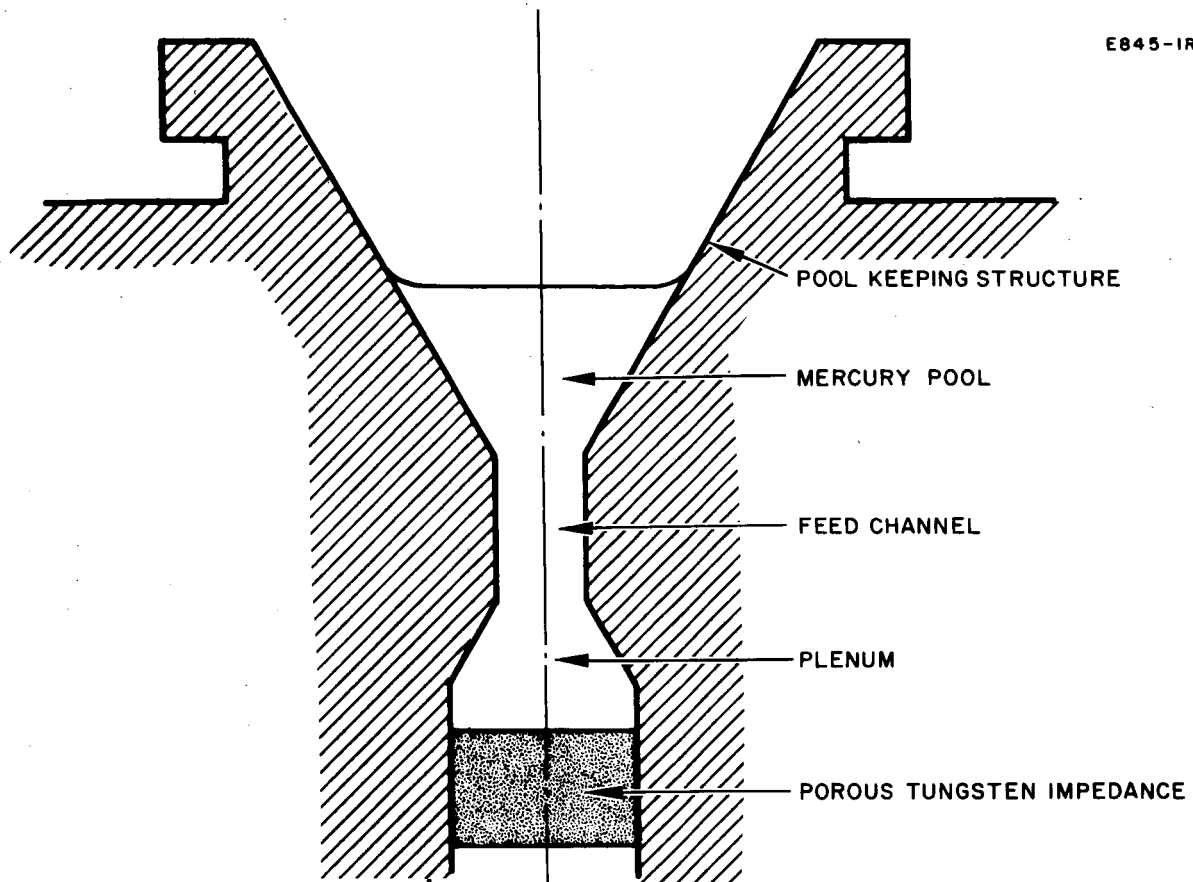


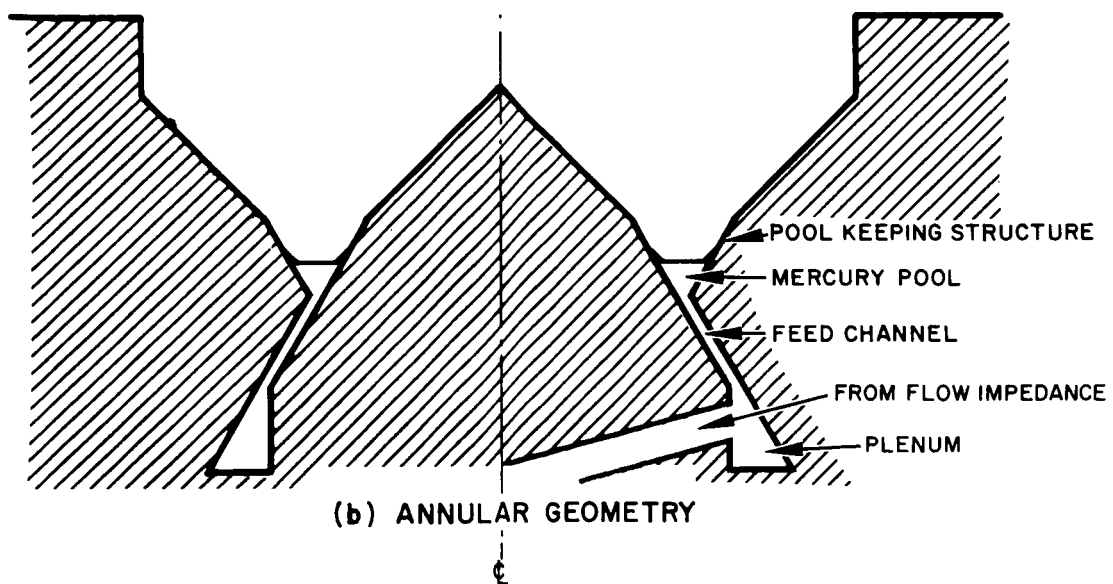
Fig. 2. Gas pressure mercury feed system.

E845-1R1



(a) CIRCULAR GEOMETRY

E845-2R2



(b) ANNULAR GEOMETRY

Fig. 3. Circular and annular cathode geometries.

perience with porous tungsten impedances has indicated that variations in fabrication are too numerous to permit exact impedance design, but rather they must be fabricated first and then calibrated to find which ones meet given requirements. Also it has been found that the flow calibrations change as a function of the past history of a given porous impedance with regard to heating, exposure to air, degree of wetting with mercury, etc. It is anticipated that these disadvantages can be overcome with the single-capillary impedance. If a constant flow calibration is established for a single-capillary flow impedance, it could serve to translate a pressure readout unequivocally into a direct, instantaneous flow rate readout.

Single-capillary flow impedances benefit also from their linear geometry in that only a small part of their active length must be in the intimate proximity of the cathode. The downstream terminus of the tube can rise to whatever cathode temperature is required for thermally integrated cathode operation, while the bulk of the impedance remains at reservoir temperature. This thermal constancy should result in repeatable and predictable flow rates which may be essential for automatic system control. Finally, it is shown in Section III that the single-capillary flow impedance offers still another advantage for use with the LM cathode through a reduction of the amplitude of mercury flow fluctuations which occur due to surface-tension forces.

C. Single-Capillary Flow Measurements

A single-capillary flow impedance was evaluated for use in the measurement and control of mercury flow to the LM cathode. The capillary consisted of a 25 cm length of type 304 stainless steel tubing having an outside diameter of 0.018 cm and an inside diameter of 0.0076 cm. The upstream end of this tube was fastened to a 1/16-in. diameter mercury feed line by means of epoxy cement. This feed line in turn was supplied with mercury by our standard piston-driven mercury feed system. The downstream end of the capillary tube discharged into a chamber which could be evacuated.

Prior to operation the capillary tube was evacuated to 10^{-3} Torr by pumping both at the open downstream end and at the mercury feed system prior to its being filled with mercury. The feed system was subsequently filled with mercury under the customary vacuum conditions.

By applying nitrogen pressure above the piston of the feed system, mercury was driven through the single-capillary flow impedance. The flow rate of mercury was accurately determined by measuring the displacement of the piston of the feed system as a function of time. Typical flow data points were acquired over periods of 30 minutes. The flow rate of mercury through the single-capillary impedance is plotted in Fig. 4 as a function of the pressure applied across the impedance. For

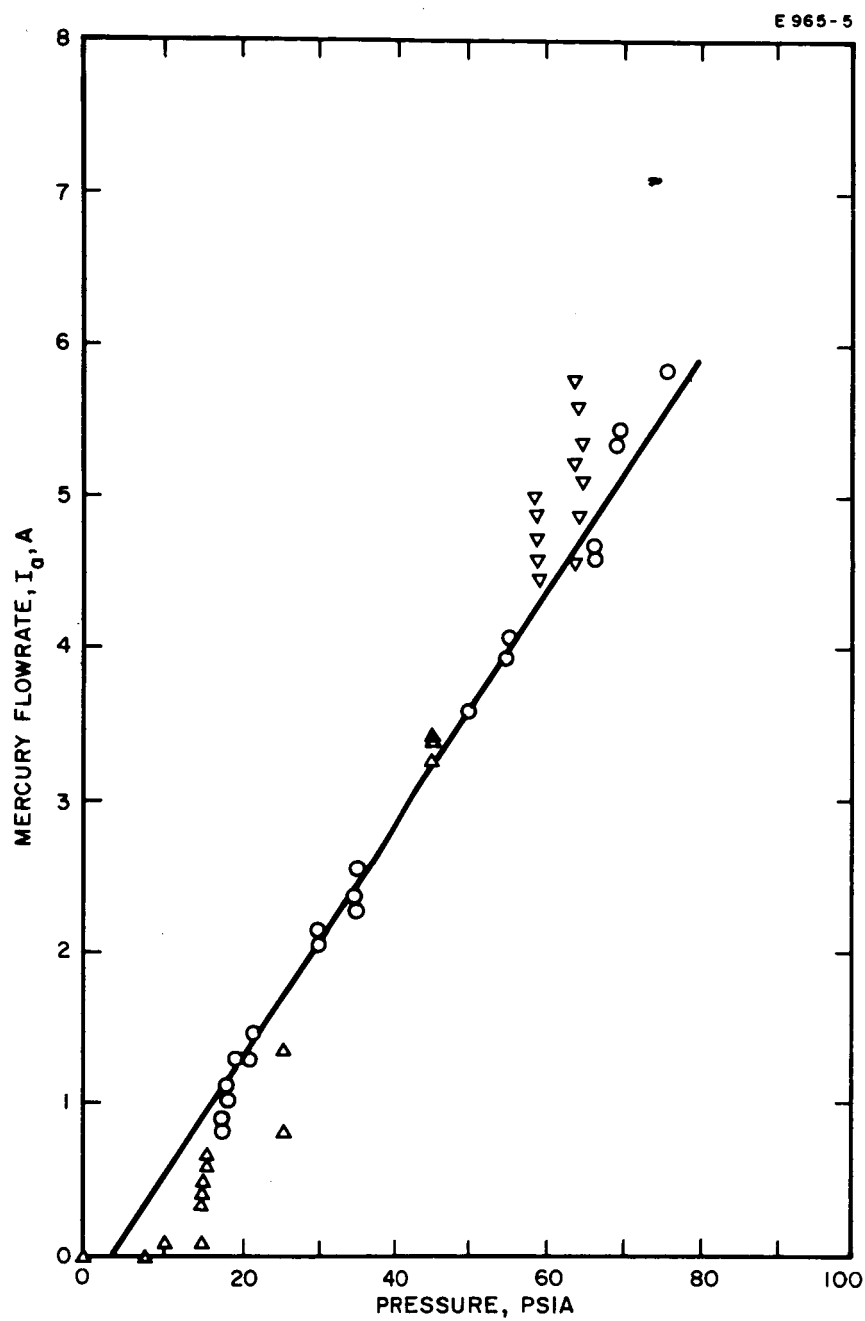


Fig. 4. Single-capillary flow impedance measurements.

changes in driving pressure to either higher or lower values within the operating range of 20-75 psia, the data points, indicated by circles, exhibit no hysteresis or other systematic variations in the flow rate. The mercury flow increased linearly with pressure at a rate of $I_a/p = 0.078 \text{ A/psia}$. Compared to a theoretically anticipated value of $I_a/p = 0.092 \text{ A/psia}$ this value is well within the tolerance anticipated from variations in tube diameter. Flow readings were both linear and repeatable as a function of pressure in this range to within the experimental error of $\pm 5\%$ at the center of the range.

Excursions beyond the stated range resulted in certain systematic variations in the flow rate. Zero flow was observed for driving pressures of less than 10 psia, and the flow was substantially reduced for a period of about 30 minutes when the driving pressure was subsequently raised to the region of 15-25 psia following such a zero-flow condition. This trend is exhibited by the data points indicated by upward-pointing triangles in Fig. 4. Similarly, when the driving pressure was returned to the operating range after having been set at 150 psia, substantially higher (+ 20%) flow rates were recorded for as long as thirty minutes thereafter. The latter trend is exhibited by the data points indicated by downward-pointing triangles in the graph. These systematic variations are not understood at this time.

D. Single-Capillary Flow Impedance Design

After the initial single-capillary flow impedance test, it was decided to design and construct a full scale flow impedance for use with an experimental LM cathode. A device shown schematically in Fig. 5 has been designed in which 2.5 m of 0.01 cm I. D. tubing is wound about a spool and then totally enclosed by a standard 3/8-in. diameter mercury feed and vacuum lead-through tube. Both the upstream and downstream ends of the capillary, are attached to the feed tube with a nickel-titanium eutectic braze.

Though it is anticipated that this braze will be highly resistant to attack by mercury, the design is such that the brazing material will not be contacted by mercury at the downstream termination where the capillary feeds into the cathode. This precaution is particularly appropriate for the case of high-temperature cathode operation where corrosion and amalgamation rates are accelerated. A pressure seal is accomplished at this junction directly between the stainless steel capillary tube and the molybdenum cathode body, the braze material being used only to attach the capillary mechanically to the center of the 3/8-in. feed tube so that the capillary tube can be pressed against the molybdenum cathode surface. The capillary impedance seals to the cathode at the upstream end of the minimum diameter flow channel which precedes the divergent-nozzle pool-keeping structure. This provides a minimum-sized mercury

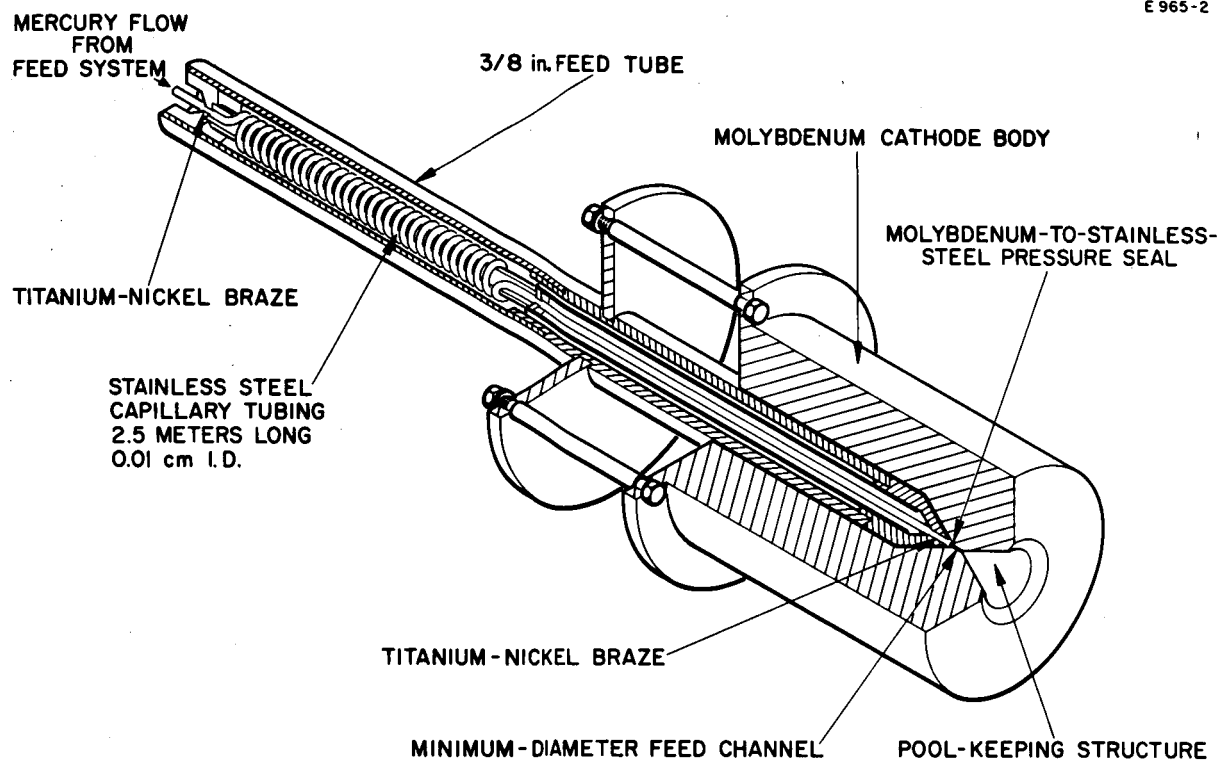


Fig. 5. Experimental cathode with single-capillary flow impedance.

plenum, and should result in excellent cathode stability for reasons which are explained in Section III.

The device shown in Fig. 5 has been fabricated and testing is presently underway. The rate of flow of mercury through the impedance is being measured as a function of the applied pressure, both to determine the calibration itself and to evaluate its constancy over a period of time.

III. LM CATHODE RESEARCH AND DEVELOPMENT

A. Introduction

Under the previous contract the annular cathode concept was adopted for high-temperature applications, in preference to the circular geometry, because it distributes the thermal cathode load $P_{K,th}$ over the circumference of the annulus (independent of the area of the mercury pool A_K) rather than around the much smaller perimeter of the corresponding circular pool. This distribution of the thermal load in the annular design serves to increase its overall thermal conductance, and operation can be achieved with much lower temperature drop between the vicinity of the mercury pool and the body of the cathode.

One drawback of the annular design is that it has been difficult to fabricate, since a feed channel with an annular gap of 2---12 μm ($0.1\text{---}0.5 \times 10^{-3}$ in) is required. Maintaining the required tolerances on the conical surfaces employed in the annular design has proved somewhat difficult, and in fact the existing annular cathodes have been fabricated with annular gaps which are no smaller than about 5 μm . As a consequence, the required electron-to-atom ratios could only be obtained at high temperature by operating these cathodes in a mode which differs from that employed at low temperatures. The mode change is indicated by the observation that the specific thermal loading of the cathode, $V_{K,th} = P_{K,th}/I_K$, is not constant as T_{Hg} is increased. Values for $V_{K,th}$ have been measured at 2.5 WA^{-1} for $T_{Hg} = 130^\circ\text{C}$, and up to 12 WA^{-1} for $T_{Hg} > 300^\circ\text{C}$. This change is due to the withdrawal of the exposed mercury surface (and hence, the arc spots) into the annular channel at higher temperatures. This mode of operation is referred to below as the retracted arc mode.

Since it is necessary to preserve the same electron-to-atom emission rates K_e/K_a when T_{Hg} is raised as for lower temperatures, the area A_K of the mercury from which evaporation takes place must be reduced (Fig. 6a and b). At the same time the annular diameter must be made as large as possible to aid in the dissipation of $P_{K,th}$ in the cathode matrix, and therefore the width of the mercury surface Δr becomes small. When Δr is reduced to the width of the feed channel ($\sim 5 \times 10^{-4}$ cm) by lowering the mercury feed pressure, further operation occurs with the cathode spot in the feed channel itself (Fig. 6c) or in fact on the surface of the mercury in the major supply channel (Fig. 6d). In this instance when A_K is again large, excessive evaporation is prevented by the feed channel itself which acts as a vapor flow constrictor, but at the same time introduces an additional voltage drop (due to the plasma losses in the channel) which is clearly detrimental to thruster performance.

E845-3RI

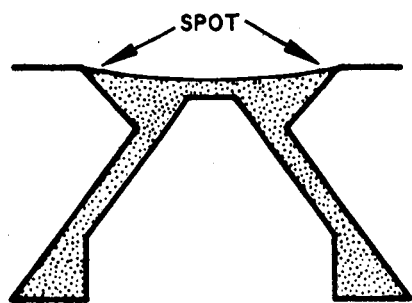
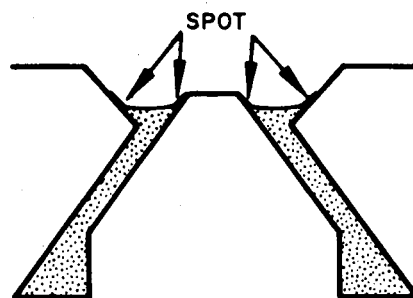
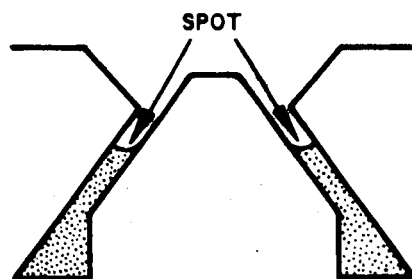
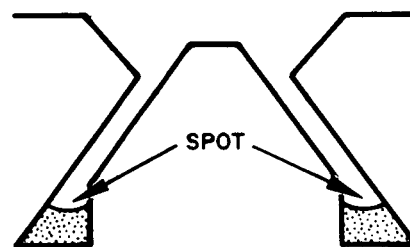
**a****b****c****d**

Fig. 6. Positions of mercury pool surface for an annular LM cathode.

To maintain low values of the specific thermal load, cathodes must be fabricated with feed channel gaps which are sufficiently small to avoid the necessity of operation of the discharge in the retracted arc mode. For the annular configuration, experience has shown that the required tolerances have not been reached by former techniques of fabrication, and greater sophistication is required to achieve them. During this quarter we have begun to undertake construction of an annular cathode which will meet design specifications.

A second area of continuing LM cathode development deals with the reduction in amplitude of fluctuations in the mercury flow rate occurring as the mercury enters the pool-keeping structure. Flow fluctuations result in corresponding fluctuations of the liquid mercury level in the pool-keeping structure. When LM cathodes are operated at high temperature or at high values of the electron-to-atom ratio K_e/K_a , the equilibrium position of the liquid level is close to the upstream end of the pool-keeping structure where the mercury surface area A_K (and therefore the rate of mercury evaporation) is minimized. In this condition, fluctuations in liquid level cause the mercury surface to recede momentarily out of the pool keeping structure and into the feed channel, which results in momentary operation in the retracted arc mode.

These fluctuations of the mercury flow rate result either from thermal fluctuations (which in turn are driven by the flow fluctuations, resulting in nonlinear oscillations with a period of ≈ 1 sec), or they result from a surface-tension instability which may occur whenever a nonwetting fluid passes through a narrow flow constriction (as explained in Section III-D). Using techniques described in Ref. 15, suitable thermal design of the pool-keeping structure and reduction in the volume of the mercury plenum (which exists between the porous tungsten flow impedance and the pool-keeping structure) have already greatly reduced the amplitude of thermally induced fluctuations. To reduce the amplitude of the flow fluctuations which may be induced by surface-tension forces, a new design principle is described in Section III-D which has been incorporated in an experimental cathode fed by a single-capillary flow impedance. All other cathodes described in Section III continue to employ a porous tungsten impedance to effect regulation of the mercury flow, since the single-capillary flow impedance is still in an experimental stage.

B. Annular Cathode Technology

During the preceding contract two annular cathodes were fabricated and designated No. 25 and No. 26. Their mean annular radii were 0.635 mm and 1.91 mm, respectively. As part of the past research effort⁵ the flow passage geometry of both cathodes was modified in several steps, the most recent of which was chosen to optimize operation in the

vapor-fed mode. In their final stages of modification neither cathode was suitable for operation in the liquid-fed mode.

During this quarter the smaller one of the two annular cathodes (No. 25) has been reworked to return it to liquid-fed operation. The mean annular radius has been enlarged to a value of 1.27 mm. The technique of assembly indicated schematically in Fig. 7 is similar to that used previously, but with one significant change which is expected to result in a considerable increase in control over the critical dimension of the narrow annular gap. As before, the two conical walls of the annular gap are machined separately and placed in the proper relative position by their own self-centering geometry. Next the two cones are lapped together to a perfect match. Then, the required annular feed channel separation is established by mating the two cones together with only a narrow tantalum shim (2.5 μ m thick) separating them (this is the new part in the assembly procedure).

Mercury is fed under pressure to a small annular plenum machined near the tip of the positive cone. It flows forward toward the tip through the narrow feed channel, into the annular pool-keeping structure which is formed by the tip of the positive cone and a small reversed negative cone which is machined in the front face of the part containing the mating negative cone. Mercury is prevented from flowing in the other direction by a metal O-ring placed midway down the positive cone. (When assembled this O-ring is crushed sufficiently so that the mating conical surfaces are separated only by the tantalum shim.) Tests with this modified cathode will be started soon.

C. Linear-Slit Cathode

The design of the linear-slit cathode is shown schematically in Fig. 8. It is based on a variation of the annular cathode concept which emphasizes the distribution of the thermal load $P_{K,th}$ over a characteristic dimension of the molybdenum cathode body rather than over the circumference of a circular liquid mercury pool. For this cathode that characteristic dimension is the 0.32-cm length of the linear slit rather than the circumference of the annulus of the annular cathode. The variation from circular to linear geometry was made in an effort to simplify the machining requirements so that greater accuracy could be achieved in fabrication. In this way sufficient control could be exercised over tolerances to insure that the feed channel is uniformly small to avoid operation in the retracted-arc mode. Similar to the technique currently employed in the assembly of the annular cathode, the feed-channel separation of the linear-slit cathode is established by inserting a 2.5 μ m thick tantalum shim between the walls on either side of the pool-keeping structure which is formed by pressing together the two cathode halves. The cathode halves are pressed together in an experi-

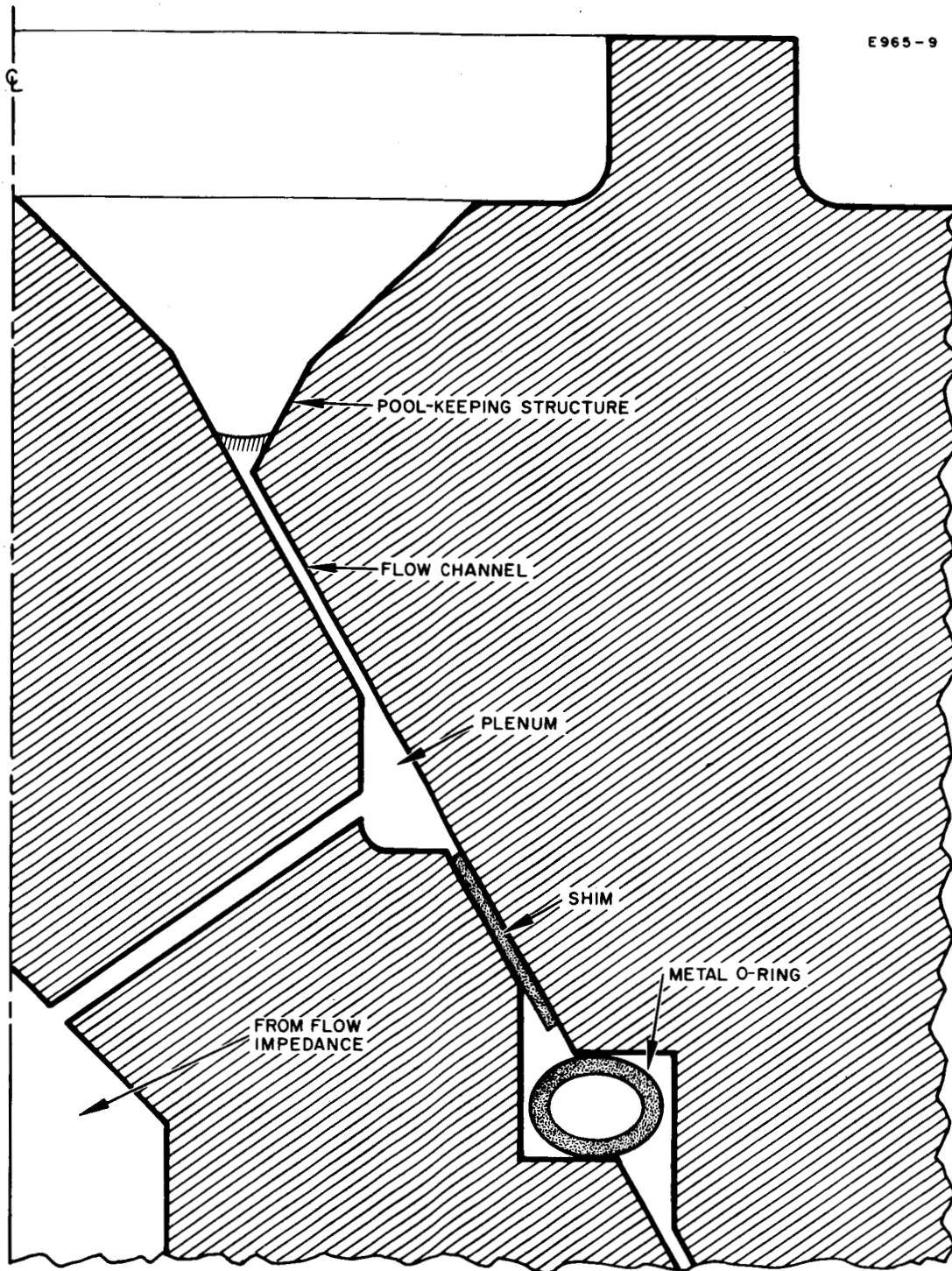
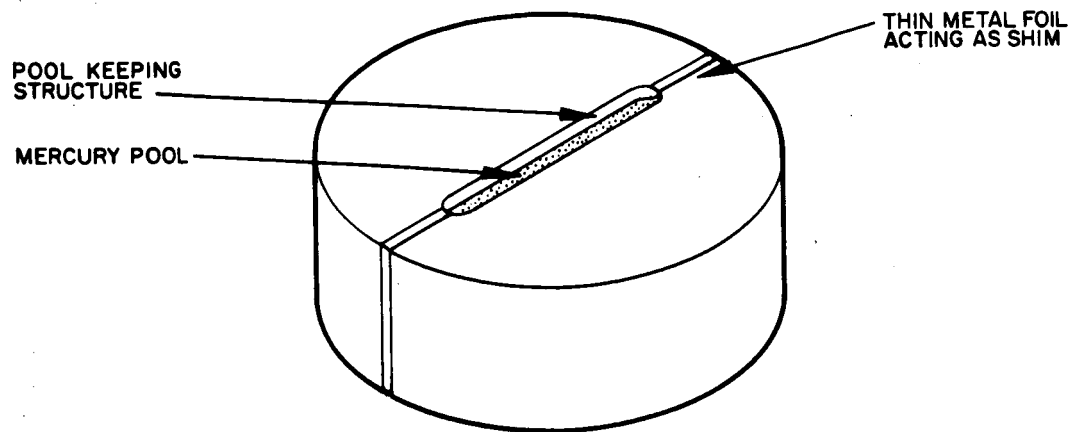


Fig. 7. Annular LM cathode using a tantalum shim to establish the feed channel width.

E845-4RI



E845-5

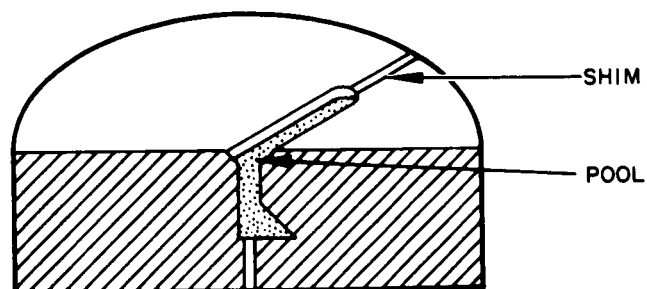


Fig. 8. Linear-slit cathode.

mental cathode mounting clamp. This clamp also contains a porous tungsten flow impedance, flow channels, seals etc., and permits rapid assessment of the performance of new pool-keeping structures.

The linear-slit pool-keeping structure has been fabricated and is presently being mounted for experimental evaluation.

D. Experimental Cathode for use with Single-Capillary Feed

Figure 5 (p. 13) shows a schematic drawing of a special cathode which has been designed to take advantage of the unique characteristics anticipated from the single-capillary flow impedance. In particular, the 60° cone of the pool-keeping structure has been extended toward a minimum diameter cross section which converges upon a 0.0038 cm diameter feed channel having a length of 0.0127 cm. This minimum diameter section of the feed channel is expected to offer an increased measure of stability from flow fluctuations which has previously been achieved only by the use of a permanently wettable metal to stabilize the position of the liquid mercury interface.

To understand the benefits derived from this design we must first understand a phenomenon which leads to fluctuations in the rate of mercury flow into the pool-keeping structures. We will assume that a steady mercury flow is provided at the entrance of the minimum diameter section of the feed channel shown in Fig. 9. The mercury passes through the feed channel and into the pool-keeping structure. The liquid in the pool-keeping structure is at a very low pressure determined by surface tension forces, by the momentum change imparted by surface evaporation of mercury atoms, and by arc pressure. Since the pressure exerted by surface tension is inversely proportional to the radius of curvature of the liquid surface,* the magnitude of the pressure due to surface tension rises greatly to a value p_{FC} within the feed channel where the radius of curvature is a minimum (the radius of curvature being equal to that of the feed channel). In the upstream direction, the pressure p_{FC} is balanced by the driving pressure of the flow system. In the downstream direction, however, p_{FC} may not be balanced and thus the downstream segment of the minimum-diameter mercury column is unstable and tends to be expelled into the pool-keeping structure. Such expulsion leaves a void, and no further mercury flow enters the pool-keeping structure until the void is filled by flow from the source, at which moment the system is again unstable and the mercury contained in the feed channel may again be expelled into the pool-keeping structure.

* This simple relationship is correct where no liquid-wall interaction occurs (i. e., nowetting) as is nearly the case with mercury on a molybdenum surface.

E965-7

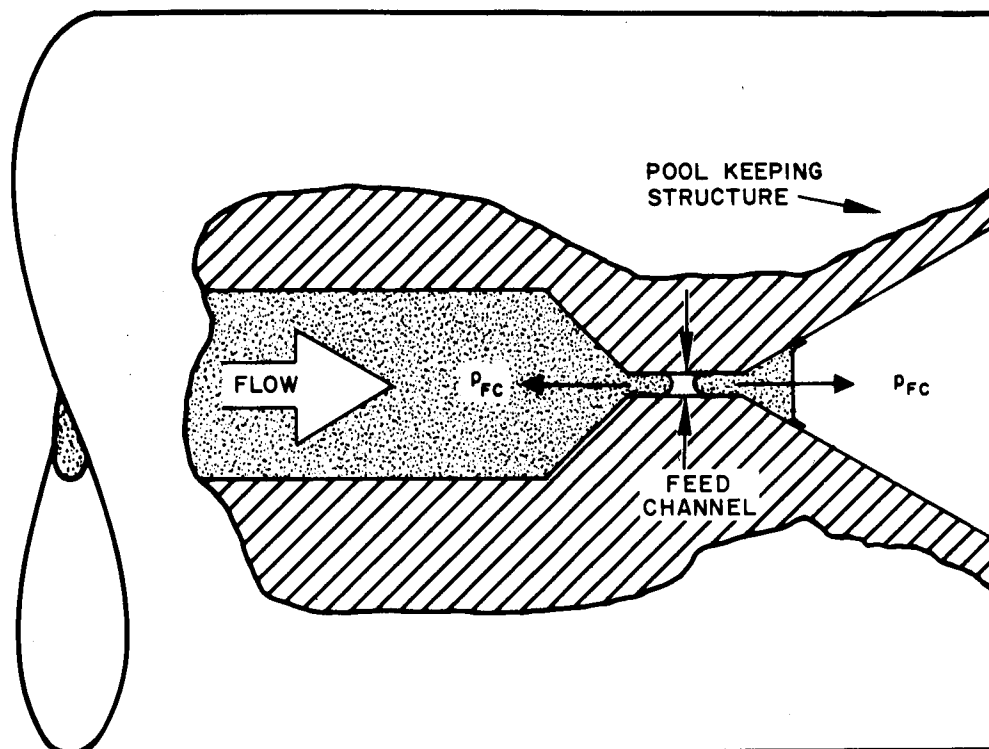


Fig. 9. Flow fluctuations due to surface-tension forces.

We see from the above description that there is a tendency for the flow of a non-wetting liquid through a small capillary to exhibit fluctuations as the liquid emerges from the capillary. We should note, however, that the point of separation of the column cannot be further upstream from the pool-keeping structure than the upstream terminus of the minimum-diameter feed channel: thus the magnitude of the flow fluctuations is limited to the volume of the minimum-diameter feed channel. The effect of these flow fluctuations can be made to be negligible so long as the volume of the feed channel is made small compared to the volume of mercury contained in the pool-keeping structure when the area A_K of the mercury surface has the desired value. The design of the cathode shown in Fig. 5 is based on this principle.

It must be appreciated that if a porous tungsten flow impedance were used in conjunction with the cathode shown in Fig. 9, then the feed channel would not present the minimum flow diameter to the mercury stream. Rather, the minimum flow diameter would occur within the pores of the impedance. Then the mercury flow entering the feed-channel would not be steady as was assumed, but would already exhibit fluctuations introduced by the porous tungsten impedance. These primary fluctuations would simply add to those introduced by the feed channel.

Only by feeding mercury to the cathode through a passage with a diameter which is everywhere larger than that of the feed channel can the fluctuation amplitude due to surface-tension forces be reduced to the minimum value imposed by the feed channel itself. To satisfy this criterion, the experimental cathode which has just been described is operated in conjunction with a single-capillary flow impedance. The design shown in Fig. 5 fulfills an even more stringent requirement: it feeds the mercury to the cathode through a passage of monotonically decreasing diameter, thereby preventing the trapping of gas bubbles. The single-capillary flow impedance also places the minimum volume of mercury in close proximity to the thermal fluctuations which can occur in the pool-keeping structure, and so minimizes the other major cause of flow fluctuations.

E. LM Cathode Neutralizer

Neutralizers based on the LM cathode principle have been described previously in the Summary Reports under Contracts NAS 3-6262¹⁵ and NASW-1404.⁵

The design of this type of neutralizer cathode is illustrated by Fig. 10. The main difference (besides size) between the neutralizer pool-keeping structure and that of the main thruster cathode is in the use of a bi-metal structure for the neutralizer. The upstream portion

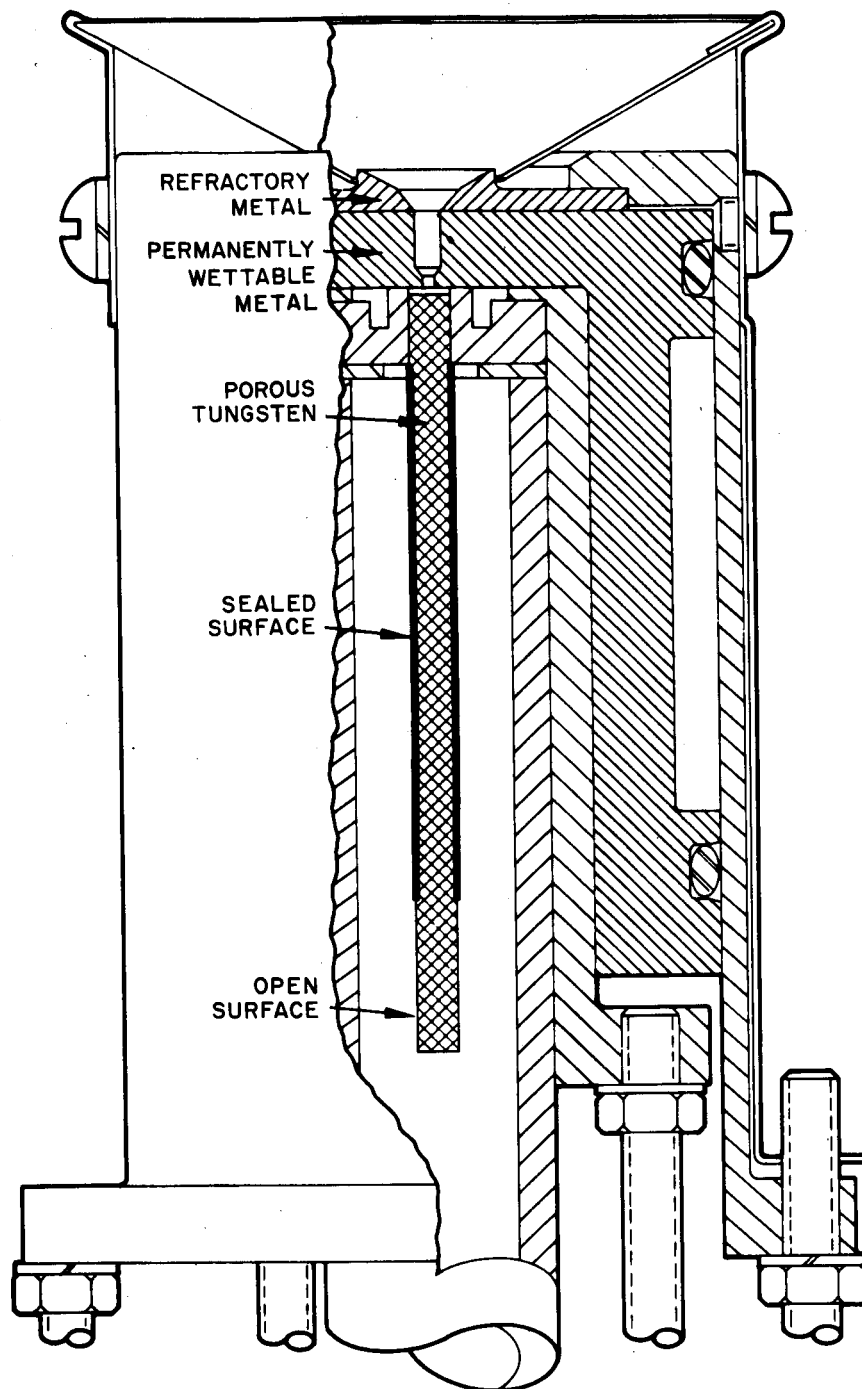


Fig. 10. Schematic cross-section of LM cathode neutralizer. (Not to scale).

consists of a metal which is permanently wettable by mercury, while the downstream portion is made of a refractory metal which requires the presence of an arc spot for each rewetting after consumption of a previous mercury layer. This combination results in the ability to contain a large-amplitude feed-rate fluctuation, while limiting the arc spot pattern excursions (under normal operating conditions) to the upstream proximity of the dividing line between the two materials, thereby maximizing the obtainable electron-to-atom emission ratio.

The materials used exclusively with this design in previously conducted tests were copper (for the upstream portion) and molybdenum (for the downstream portion). During the last three months the effort on LM cathode neutralizers was concentrated on

(a) establishing the limiting electron-to-atom ratio for this combination of materials and

(b) investigating the performance of cathodes using other materials for the upstream portion.

The results of a recent Company-supported program at HRL¹⁶ had led us to expect that considerably higher electron-to-atom emission ratios (K_e/K_a) than previously reported⁵ (≈ 115) should be obtainable. In this recent study a method has been developed which permits separate determination of the efflux of mercury atoms from the arc spots ($K_{a,s}$) and of the efflux due to evaporation from the inactive mercury surface ($K_{a,v}$). It was found that $K_e/K_a \approx 200$, independent of current over the range of measurement (15 to 60 A).

It seemed justified to expect the same value of $K_e/K_{a,s}$ also for the neutralizer current range, and we were confident that our neutralizer cathode design would permit us to keep $K_{a,v} \ll K_{a,s}$, so that $K_e/K_a \approx K_e/K_{a,s}$. A copper-molybdenum neutralizer, having a pool-keeping structure with 0.25 mm diameter cylindrical bore, was selected to test the validity of this extrapolation. An operating temperature of 40°C was found to give the best compromise between low $K_{a,v}$, requiring low temperature, and avoidance of mercury recondensation on the downstream portion of the pool-keeping structure, which requires a relatively high temperature. (Such recondensation, similar to splashing,^{5,15} leads to frequent arc extinctions in the neutralizer current range).

When all parameters were optimized, it was indeed found possible to operate this cathode at $K_e/K_a \approx 200$ (average for a 2-hour run), with a current of 1.9A and a diode discharge voltage of ≤ 30 V. While this result was achieved under strictly laboratory conditions and does not represent performance readily available on a thruster in space, it does demonstrate the ultimate potential of this approach and it confirms our predictions.

The results of the evaluation of materials for the upstream portion of the pool-keeping structure can best be represented by the following table:

Platinum	↑ Excessive amalgamation, resulting in some consumption of structural material.
Aluminum	
Copper	Best overall performance of materials tested.
50% porous tungsten, filled with copper	↓ Insufficient permanent wettability, resulting in instability of arc spot anchoring at low currents.
Cold rolled steel	
Iron	
Stainless steel (304)	
Tungsten	
Nickel	
Tantalum	

(The arrows indicate the direction of increasing importance of the state properties.)

For the materials listed closest to copper, several days of continuous operation were required to reveal an inferiority compared to copper, while for the most extreme entries the deficiency became obvious after a few minutes of operation.

IV. LM CATHODE THRUSTER OPTIMIZATION

A. Introduction

While the performance of the LM cathode itself can for the most part be determined by operation in a diode discharge, the performance requirements which must be met by the cathode can only be established by operation of the LM cathode in a thruster. Though separate programs have been conducted at LeRC to optimize the 15-cm SERT II thruster for operation with both the oxide⁷ and the hollow-cathode,⁸ no similar data are available for operation of an LM cathode in a similarly optimized thruster. No LM cathode thruster optimization program has been undertaken since November 1966.) At their present state of development, the various cathode types (i. e., oxide, hollow, and LM) are not simply interchangeable within a given thruster; therefore the SERT II performance data can not apriori be used to set the requirements for LM cathode performance. Thus it is necessary to conduct a separate program to optimize the Kaufman thruster for operation with the LM cathode.

Improvements achieved in discharge chamber performance are important both as an enhancement of LM cathode thruster efficiency and also because they represent a relaxation of the demands on performance from the LM cathode. The latter point can be illustrated by examining the dependence on thruster performance of one of the parameters which has been important in the development of the LM cathode: the electron-to-atom ratio K_e/K_a . The value of this parameter which is required for given thruster operation is equal to

$$K_e/K_a = \eta_m \frac{I_K}{I_B},$$

where η_m is the mass utilization, I_K is the cathode discharge current, and I_B is the beam current. In the LM cathode thruster the product of the discharge voltage V_D times the ratio of cathode to beam current is simply equal to the source energy required to produce an ion, V_S :

$$V_D \frac{I_K}{I_B} = V_S$$

Combining the above two expressions we have

$$K_e/K_a = \eta_m \frac{V_S}{V_D}.$$

We see from the final expression that for a given value of mass efficiency and constant discharge voltage, the ratio K_e/K_a depends directly on the source energy per ion.

Previous LM cathode thruster performance of $V_S = 400$ eV/ion at $\eta_m = 87\%$ reported in Ref. 5 required values of $K_e/K_a \approx 10$. This corresponds to a ratio of cathode discharge current to the thruster beam current $I_K/I_B \approx 12$. Improvement of thruster performance to a level of $V_S = 200$ eV/ion for the same discharge voltage reduces the requirements to $K_e/K_a \approx 5$ and $I_K/I_B \approx 6$. The lower value of K_e/K_a permits design of LM cathodes having feed channels with twice the width previously required for non-retracted operation. The lower value of I_K/I_B specifies that only half as much thermal power P_K , is delivered to the cathode per unit beam current.

B. Modification of 20-cm PMT

As a first step in a program to optimize the Kaufman thruster for operation with the LM cathode, an existing 20-cm diameter permanent magnet thruster (PMT) was modified to conform (in first approximation) to the magnetic field geometry of the LeRC 15-cm SERT II thruster. The present configuration of this thruster is shown schematically in Fig. 11 which is approximately to scale. It was equipped with a magnetic collar and with both screen and cathode pole pieces to reproduce the desired magnetic field profile. A baffle was placed downstream of the cathode pole piece by a variable axial distance d . The exact configuration of this baffle was modified in a series of separate experiments.

The design of the baffle configurations was guided by the magnetic-shadow technique enunciated during our previous thruster optimization effort^{4, 15} in which the tailored distribution of electrons over the discharge chamber cross section by means of a baffle was introduced. With this technique, a baffle (with or without apertures) is placed downstream of the cathode, so that electrons streaming around the baffle perimeter or through the apertures emerge on and follow magnetic field lines which intersect the screen electrode at radii selected to yield maximum over-all thruster performance. A further function served by the baffle (which became clear in more recent studies^{5, 8} and during the current effort is to constrict the passage of electron flux from the cathode to the discharge chamber. This permits the discharge voltage to be raised to any desired level, thus allowing an independent choice of discharge voltage as a parameter in thruster optimization.

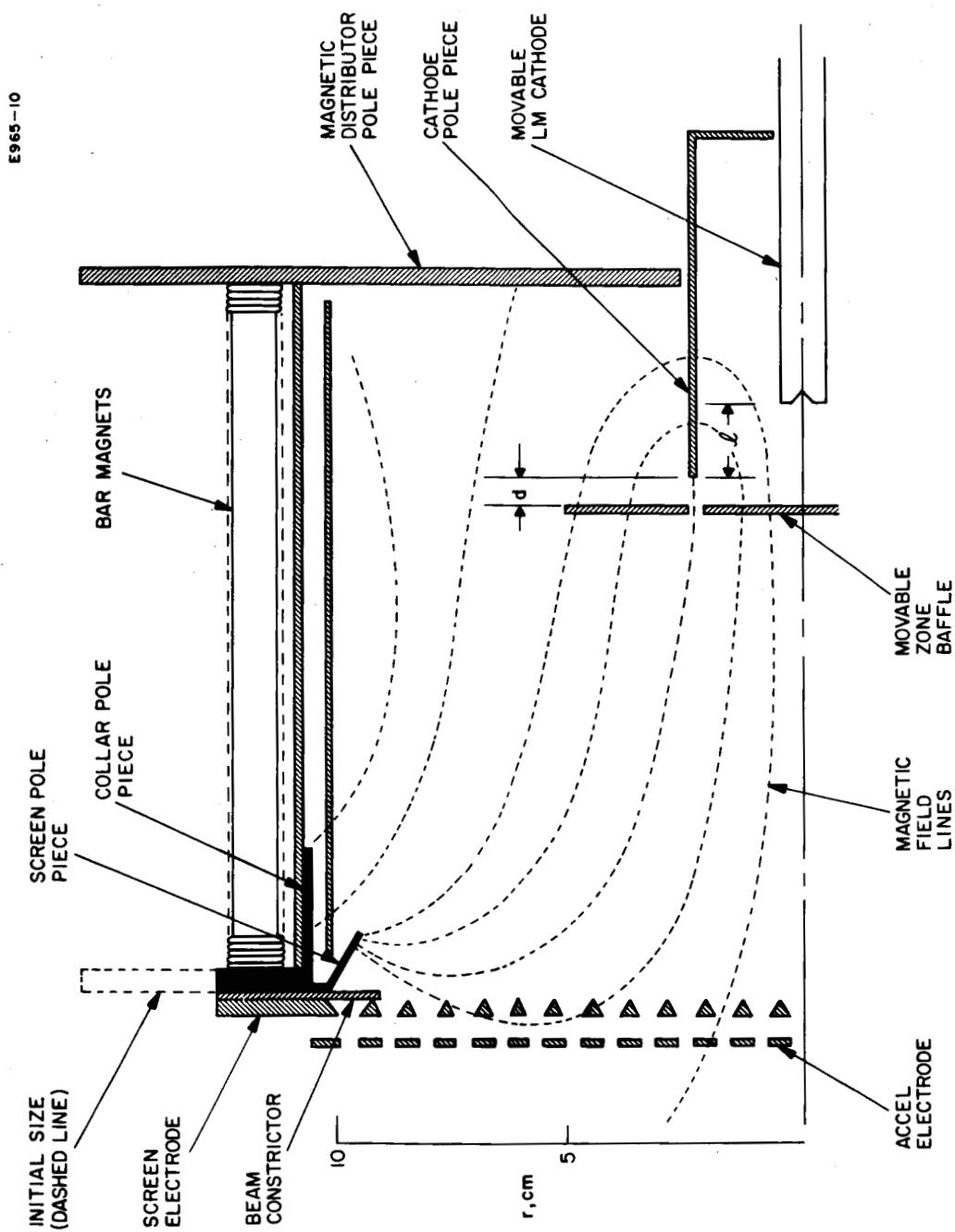


Fig. 11. Present configuration of the modified 20-cm PMT.

The cathode was placed at an axial distance l behind the mouth of the cathode pole piece; this dimension was also variable. All of the propellant was fed through the cathode in deviation from the technique used in the SERT II thruster.

Iron-filing magnetic field plots demonstrate that the SERT II field is reasonably approximated. Initially, the wire-wound simulated permanent magnets were located several centimeters beyond the radius of the iron collar, but they were moved in close to the collar for the last several experiments to the position shown in Fig. 11. In the final experiment conducted to date, a beam-constricting electrode was employed to reduce propellant loss from the outermost screen apertures.

The first four experiments established the typical operation of the initial configuration before the magnets were moved close to the collar and the beam constricting electrode was employed. The results of these tests are displayed in Fig. 12 and summarized in Table I.

E965-6RI

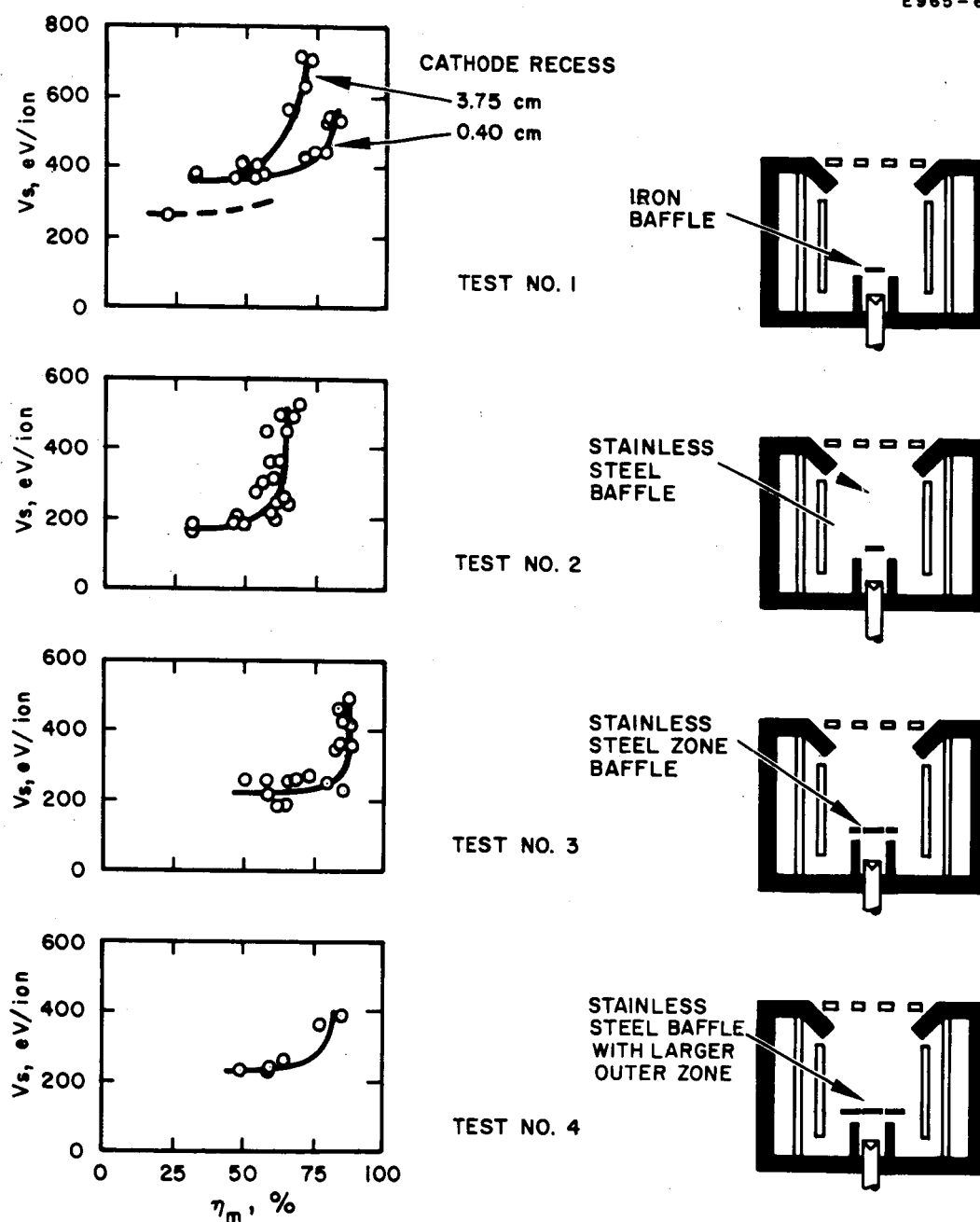


Fig. 12. Experimental data for the modified 20-cm PMT with various baffle configurations.

Table I: Typical operation of modified 20-cm PMT with various baffle configurations.

Test No.	Baffle Configuration	Results
1	As described above with 2.93 mm annular gap between the O.D. of the cathode pole piece and the I.D. of the <u>iron</u> baffle.	The discharge voltage was $V_D \approx 30$ V. Performance was improved by varying the cathode position from $\ell = 3.75$ cm to $\ell = 0.4$ cm. Best operation was achieved with the baffle located at $d = 1$ cm. Almost constant source energy per ion $V_S \approx 360$ eV/ion for mass efficiency $34\% < \eta_m < 60\%$, then rising. Separate low power mode of $V_S = 250$ eV/ion noted at $\eta_m \approx 22\%$.
2	As described above, but with a 1.46 mm annular gap between the cathode pole piece and a <u>stainless steel</u> baffle.	The discharge voltage was $V_D \approx 28$ V. Operated only in low-energy mode. Critically dependent on magnetic field intensity and baffle position. Two performance peaks, one with baffle located at $d = 0.5$ cm, the other at $d = 1.8$ cm downstream of end of cathode pole piece. Performance was not critically dependent on cathode position for $1 \text{ cm} < \ell < 3 \text{ cm}$. $V_S < 200$ eV/ion for $32\% < \eta_m < 55\%$, rising steeply at $\eta_m = 60\%$.
3	As described in Test No. 2, but with a stainless steel annular baffle in the same plane and surrounding the central disk [4.7 cm I.D. (equal to the inner diameter of the cathode pole piece), and 10.1 cm O.D.]	The discharge voltage was $V_D \approx 35$ V. Best performance was achieved with the baffle located at $d = 0.4$ cm downstream of end of cathode pole piece. Performance was not critically dependent on cathode position for $1 \text{ cm} < \ell < 3 \text{ cm}$. $V_S \approx 200$ eV/ion for $52\% < \eta_m < 80\%$, rising sharply at $\eta_m = 85\%$.
4	As described in Test No. 2, but with a larger stainless steel annular baffle in the same plane and surrounding the central disk (4.7 cm I.D., 18 cm O.D.)	The discharge voltage was $V_D \approx 30$ V. Best performance was achieved with the baffle located at $d = 0.4$ cm downstream of end of cathode pole piece. Performance was not critically dependent on cathode position for $1 \text{ cm} < \ell < 3 \text{ cm}$. $V_S \approx 240$ eV/ion for $\eta_m < 70\%$, rising thereafter.

Subsequent to the completion of these four experiments, the magnets were moved radially inward to a position close to the collar pole piece. Little change in performance was noted in response to this change. The magnetic field lines shown in Fig. 11 were measured with the magnets placed in this configuration. Of these first four experiments, the most promising performance resulted from test No. 3. The major deficiency which was apparent from this configuration was a rather precipitous rise in source energy per ion V_S occurring at $\eta_m \approx 85\%$, as though the thruster had reached a premature saturation in propellant utilization. It was presumed that the most probable cause of the indicated saturation was a loss of propellant occurring at the outermost apertures of the screen electrode. These apertures are partially shielded from the plasma by the screen pole piece, and can not be expected to produce intense beamlets, but are able to pass neutral particles arriving from the chamber and from recombined ions leaving the screen pole piece.

While using the baffle configuration of test No. 3, a non-magnetic beam constrictor was placed upstream of the screen electrode, thereby restricting the beam diameter to 18 cm in order to reduce the loss of neutral particles from the outermost apertures. The data shown in Fig. 13 for this configuration represents the best performance obtained to date. Each of the three data points which is presented represents an average of data which was taken over a period of from 45 minutes to two hours of thruster operation. Optimum performance was obtained with the baffle placed 1-2 mm downstream of the end of the cathode pole piece, and was not sensitive to the position of the cathode within the cathode pole piece. The discharge voltage was maintained at an optimum value $V_D \approx 35$ V, which was set by adjustments of the baffle position and of the magnetic field intensity. Discharge chamber performance was not critically dependent on mass flow rate (the data presented in Fig. 13 was obtained at a mass flow equivalent of $I_a = 650$ mA). For optimum performance the magnetic field intensity had a value $B \approx 30$ G on the axis at the midplane of the discharge chamber. Some penalty was paid for the use of the constrictor as evidenced by a slight rise, in the minimum source energy to a value $V_S \approx 240$ eV/ion. The benefit of the constrictor, however, is clearly evident by the increased mass utilization.

This present modification of the 20-cm PMT has achieved an immediate goal of establishing design criteria for construction of a new 30-cm Kaufman thruster which will serve as the performance-optimized test vehicle for future LM cathode development.

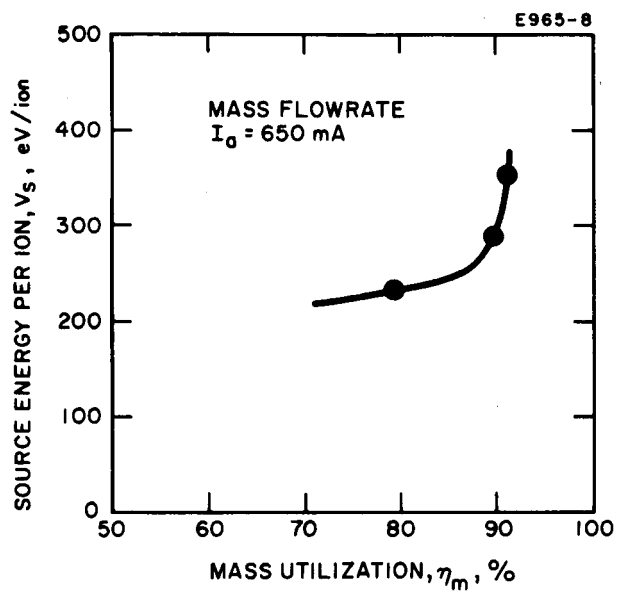


Fig. 13. Experimental data for modified 20-cm PMT (present configuration).

C. Design of 30-cm PMT

A 30-cm permanent-magnet thruster has been designed to serve as a test vehicle for LM cathodes and related systems being developed under this contract. This design borrows heavily from geometrical criteria evolved in the recent optimization of the NASA 15-cm SERT II thruster for LeRC.^{7,8,9} The initial baffle geometry and operating techniques will be derived from the experimental development already nearing completion utilizing the modified 20-cm PMT and will be optimized from that point by operation within the 30-cm thruster.

A schematic drawing of the 30-cm thruster design is shown in Fig. 14. The anode diameter of 30 cm is twice the value used for the SERT II thruster. The screen and cathode pole pieces, the magnetic collar and magnetic distributor pole pieces are all scaled up by the same factor. The separation between the anode and the thruster shell has not been increased from the SERT II dimension, and the overall length is 20 cm. The total weight of the basic thruster as shown in Fig. 14 is calculated to reach approximately 4.7 kg.

The anode is attached to an external connector by a series of lead-throughs consisting of short aluminum rods which pass through insulating ceramic sleeves. These lead-throughs serve not only to connect the anode to the external electrical circuits, but also pass the discharge heat delivered to the anode on to the external connector. By virtue of this arrangement, it has been calculated that for a source energy per ion $V_S = 200$ eV/ion the anode will operate at an equilibrium temperature of 300°C for thrusters clustered in a peripheral array. Under these conditions, the cathode is calculated to operate also at a temperature of 300°C while rejecting its own thermal load along a tapered aluminum backplate to the outer thruster shell where it is radiated away at a temperature of 150°C . This calculation is based on demonstrated values of cathode performance given in Ref. 5, typically exhibiting a specific thermal load of $V_{K,th} = 7.5$ W/A for an LM cathode operating temperature of 300°C . The analysis on which these calculations are based has assumed that radiation is permitted only from the thruster side wall, and that there is no heat shielding between anode and cathode surfaces. It is anticipated that forthcoming advances in high-temperature LM cathode technology will significantly lower the heat load to the cathode, resulting in the possibility of a further thruster weight reduction.

The design of the 30-cm PMT is based on the use of aluminum as the major structural material. This metal was chosen for this application because of its almost unique combination of extreme light weight and high thermal conductivity, which together have resulted in the design of a light-weight thermally integrated thruster.

E96b-1

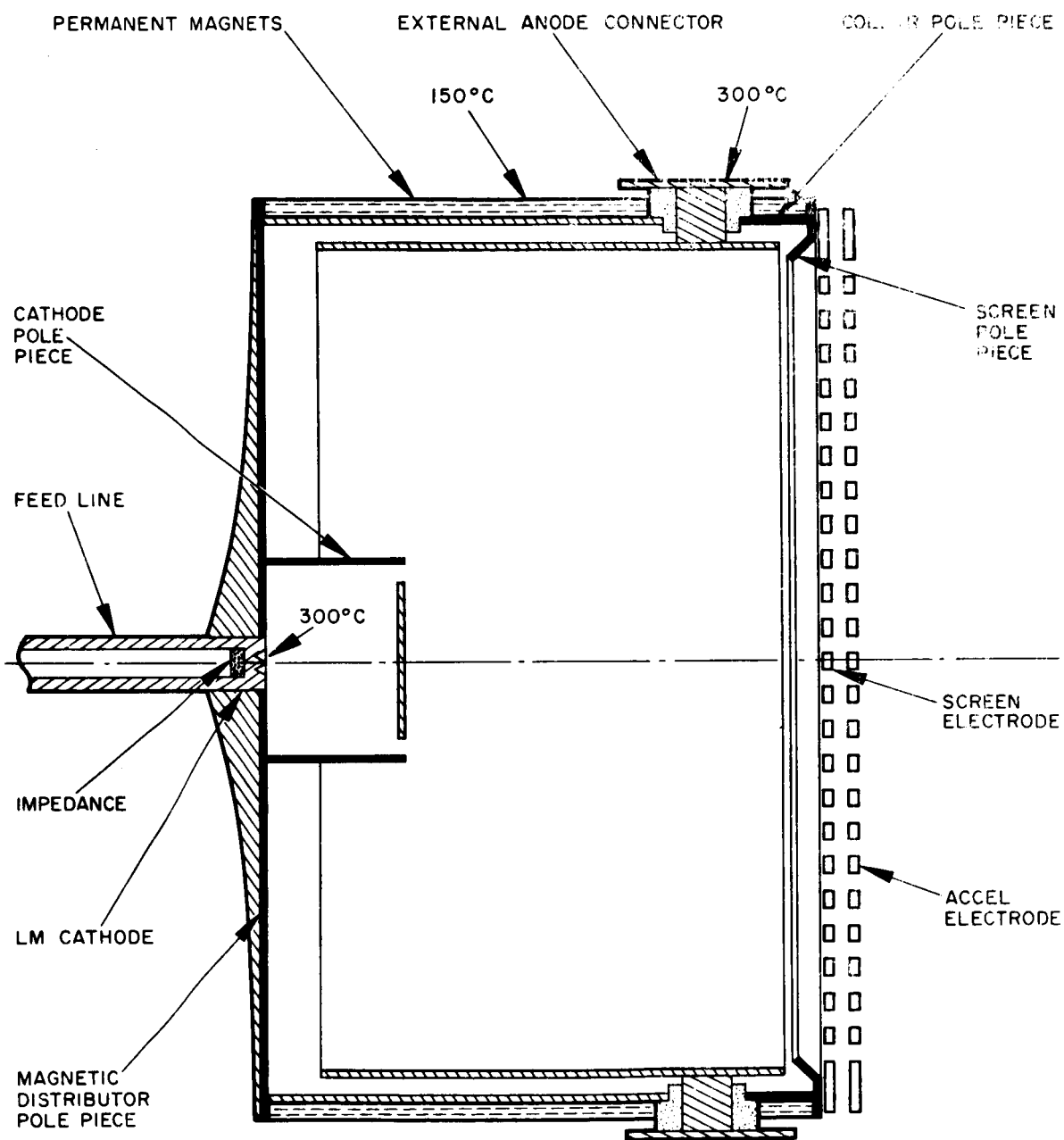


Fig. 14. Schematic drawing of the 30-cm PMT design.

The literature shows no explicit data to indicate the compatibility of aluminum with mercury over the typical range of operation of an electron-bombardment thruster (475-675°K at a mercury vapor pressure of about 10^{-4} Torr). At normal atmospheric conditions, aluminum is reported^{17, 18} to be a poor structural material in the presence of mercury. It has recently been found in this laboratory in work done under a NASA contract (NAS 3-9703) that high purity aluminum may be resistant to or alternatively may be attacked by mercury depending on other environmental parameters. Briefly, an aluminum ribbon electromagnet when kept at approximately 200°C in mercury vapor at a pressure of 10^{-4} Torr has not suffered deterioration over a period of some 500 hours. This anodized ribbon is stripped of the aluminum oxide on its ends in order to make electrical contacts. Any attack on the thin ribbon would become apparent immediately since a local attack would increase the incremental resistance of the ribbon at that point. This would result in a hot spot, which in turn would accelerate the attack and the destruction of the coil in that area. When the same coil is placed in an environment consisting of normal room atmosphere and drop size concentration of liquid mercury on the surface, attack occurs immediately on the stripped portion. The reason for the onset of mercury attack is not understood, but may possibly be due to the addition of room water vapor to the aluminum-mercury galvanic couple.¹⁹ These observations rule out the use of commercial purity aluminum in the fabrication of structural components of thrusters which must undergo laboratory testing.

When considering aluminum alloys which possess ample strength for ion engine structures, the literature shows several pertinent points. An attack²⁰ of the stress corrosion type takes place on some 2000 and 7000 series aluminum alloys. Scratching or removing the protective oxide film is also reported²¹ to render alloys vulnerable to mercury attack. On the other hand, it has been observed²² that 3-5% silicon alloys resist cold mercury attack and have considerable resistance to hot mercury vapor. This conclusion is borne out by our experience at this laboratory that 6061 aluminum (a low silicon alloy) vacuum chamber end plates at room temperature have not been affected by exposure to 10^{-4} Torr mercury pressure over a period of four years. They have also resisted attack due to droplets of mercury which accumulate on parts mounted on the plates and drip down during assembly or disassembly. This observation seems to negate the vulnerability of this aluminum alloy to mercury when scratched since they are handled without any regard for scratching.

From these observations made at HRL and from the statements found in the literature, it appears reasonable to expect that 6061 aluminum alloy can serve successfully as the major structural material in the fabrication of the 30-cm PMT. We have definite knowledge that this alloy has resisted attack by mercury droplets lying on the surface

when the metal is exposed to normal atmospheric conditions, and we have reason to believe that it can also resist attack under the thruster operating environment of 475-675°K at a mercury vapor pressure of 10^{-4} Torr. The decision to fabricate the thruster from this alloy must be considered as an experiment which will be of significant value in itself since it will answer a question of general importance for the development of electron-bombardment thrusters. While this choice has been made, research on the compatability of aluminum alloys with the thruster environment will continue.

V. CONCLUSIONS

We have started an effort of research and development to consolidate the benefits which can be derived from recent experimental advances in electron-bombardment thruster operation at HRL, JPL, and LeRC, and to apply these to the task of optimizing the electron-bombardment thruster for operation with an LM cathode. We also expect to reap the benefits indicated by past analytical studies with regard to the thermal integration of the thruster system with respect to the LM cathode. Only by operating the cathode in an optimized thruster can realistic demands be established for LM cathode performance.

In parallel with the development of an electron-bombardment thruster which is optimized for use with the LM cathode, research and development continues on the cathode itself, as well as on many of the auxiliary components which are necessary to produce a workable thruster system.

Accomplishments to date include:

1. Measurements of Poiseuille flow of mercury through a single-capillary flow impedance were linear and repeatable to within the experimental error of $\pm 5\%$ (in the range of interest for electron-bombardment thrusters.)
2. An experimental LM cathode has been constructed which is fed by a single-capillary flow impedance.
3. A new technique has been introduced for the assembly of LM cathodes which employs the use of shims to establish the uniformly small feed channels desired for high-temperature operation. This technique has been applied to the annular LM cathode and to a new linear-slit LM cathode.
4. An LM cathode neutralizer has been operated (under strictly laboratory conditions) at $K_e/K_a \approx 200$ with a current of 1.9 A and a diode discharge voltage of ≤ 30 V.
5. A modified 20-cm permanent magnetic thruster has been operated with the following performance:

Beam Current	-	$I_B = 550$ mA
Source Energy per Ion*	-	$V_S = 250$ eV/ion
Mass Utilization	-	$\eta_m = 85\%$

* V_S is the total energy required to form an ion, since no heater, vaporizer, or keeper power is required with the LM cathode.

6. A 30-cm permanent magnet thruster design is now complete which attempts to exploit the experience gained through recent development of optimized thrusters at HRL, JPL, and LeRC. This thruster incorporates features necessary for thermal integration of the cathode within the overall thruster system and is calculated to weigh approximately 4.7 kg.

VI. RECOMMENDATIONS AND FUTURE PLANS

Continuation of the program is planned along the following lines:

- Study of techniques of mercury flow measurement and control, and of high-voltage isolation. Operation of the previously developed hydrogen-bubble high-voltage isolator in conjunction with an LM cathode to demonstrate their compatibility. Continuation of measurements of Poiseuille flow through single capillary tubes, and initiation of experiments to determine the cause of the systematic flow variations which have been observed.
- Testing of several new cathodes, including
 1. The reworked annular cathode No. 25 using the shim assembly technique.
 2. A linear-slit cathode.
 3. An experimental cathode employing a single-capillary flow impedance.
 4. LM neutralizer cathodes employing new combinations of material in their pool-keeping structures.
- Construction of 30-cm thruster.

VII. NEW TECHNOLOGY

During this reporting period, one invention which is believed to be patentable has been reduced to practice. (This invention had been conceived prior to the Contract start date.) The patent docket number, title, and name of inventor are as follows:

PD 68277 LM Cathode with a Single-Capillary Flow Impedance, by Julius Hyman, Jr.

The principles on which this invention is based are first reported to NASA in Section II-D of this Quarterly Report, dated May 15, 1968. The disclosure is in the process of being forwarded to NASA by the Corporate New Technology Director.

VIII. REFERENCES

1. W. O. Eckhardt, "Liquid-Metal Arc Cathode with Maximized Electron/Atom Emission Ratio," patent applied for.
2. W. O. Eckhardt, J. A. Snyder, H. J. King, and R. C. Knechtli, "A New Cathode for Mercury Electron-Bombardment Thrusters," AIAA Paper No. 64-690, August 1964.
3. H. R. Kaufman: "An Ion Rocket with an Electron Bombardment Ion Source," NASA TN D585, January 1960.
4. W. O. Eckhardt, H. J. King, J. A. Snyder, J. W. Ward, W. D. Myers, and R. C. Knechtli: "4000-hr Life Test of a Liquid-Mercury Cathode in a 20-cm LeRC Ion Thruster," Special Report Contract NAS 3-6262, Oct. 1966; also: H. J. King, W. O. Eckhardt, J. W. Ward, and R. C. Knechtli: "Electron-Bombardment Thrusters using Liquid Mercury Cathodes," J. Spacecraft 4, 599 (1967).
5. W. O. Eckhardt, K. W. Arnold, G. Hagen, J. Hyman, Jr., J. A. Snyder, and R. C. Knechtli: "High-Temperature Liquid-Mercury Cathodes for Ion Thrusters," Summary Report Contract No. NASW-1404, July 1967.
6. W. O. Eckhardt, H. J. King, J. A. Snyder, and R. C. Knechtli: "Liquid-Metal Cathode Research," AIAA Paper #66-245, March 1966.
7. R. T. Bechtel, "Discharge Chamber Optimization of the SERT II Thruster," AIAA Paper No. 67-668.
8. R. T. Bechtel, G. A. Csiky, and D. C. Byers, "Performance of a 15-cm Diameter, Hollow-Cathode Kaufman Thruster," NASA TM X-52376.
9. W. R. Kerslake, D. C. Byers, and J. F. Staggs, "SERT II Experimental Thruster System," AIAA Paper No. 67-700.
10. H. J. King, "Oxide Cathode Mercury Thruster Systems," Research Report No. 374, June 1967, Hughes Research Laboratories, Malibu, California.
11. W. Knauer and R. L. Poeschel, "Discharge Chamber Studies for Mercury Bombardment Thrusters," Semi-Annual Report, Contract No. NAS 3-9703.

12. Private Communication with Paul D. Reader and Eugene V. Pawlick of JPL, 1968.
13. J. H. Molitor, H. J. King, and S. Kami, "A Study of Liquid Mercury Isolator Development," Sept. 1967, Final Report, Contract No. NAS 7-539.
14. Private Communication with Paul D. Reader of JPL, 1968.
15. W. O. Eckhardt, H. J. King, J. A. Snyder, J. W. Ward, W. D. Myers, and R. C. Knechtli: "Liquid-Mercury Cathode Electron-Bombardment Ion Thrusters," Summary Report Contract No. NAS 3-6262, Oct. 1966.
16. G. Eckhardt, "Efflux of Mercury Atoms from the Cathode Spots of the Low-Pressure Arc," Paper to be presented at the Third International Symposium on Discharges and Electrical Insulation in Vacuum, Paris (September 1968).
17. Liquid Metals Handbook, U. S. Government Printing Office, 2nd Ed. 165, (June 1954).
18. J. Nejedlik and E. Vargo, "Material Resistance to Mercury Corrosion," Electrochemical Technology, Vol. 3, No. pp 9-10, 250 (1965).
19. W. Latimer & J. Hildebrand, Principles of Chem. & Refer. Book of Inorg. Chem. Macmillan Co., p. 90, 1940.
20. H. Logan, The Stress Corrosion of Metals, Wiley & Sons, p. 193, 1966.
21. H. Uhlig, The Corrosion Handbook, Wiley & Sons, p. 618, 1948.
22. B. Power & F. Robson, "Experiences with Demountable U.H. V. Systems," Tech. Rep. of Edwards High Vacuum Ltd., Crawley, Sussex, England.